

1 **Artificial intelligence assisted standard white light**  
2 **endoscopy accurately characters early colorectal cancer: a**  
3 **multicenter diagnostic study**

4 Sijun Meng<sup>1</sup>, MD, PhD, Yueping Zheng<sup>2</sup>, MD, Ruizhang Su<sup>2</sup>, MD, Wangyue Wang<sup>3,4</sup>, MD, Yu Zhang<sup>3</sup>,

5 MD, PhD, Hang Xiao<sup>5</sup>, PhD, Zhaofang Han<sup>6,7</sup>, PhD, Wen Zhang<sup>8</sup>, PhD, Wenjuan Qin<sup>2</sup>, PhD, Chen

6 Yang<sup>5</sup>, PhD, Lichong Yan<sup>9</sup>, PhD, Haineng Xu<sup>10</sup>, PhD, Yemei Bu<sup>5,11</sup>, MS, Yuhuan Zhong<sup>12</sup>, PhD, Yi

7 Zhang<sup>13</sup>, MD, Yulong He<sup>1</sup>, MD, PhD, Hesong Qiu<sup>6</sup>, MD, MBA, Wen Xu<sup>12</sup>, PhD, Hong Chen<sup>1</sup>, MD,

8 Siqi Wu<sup>6,14</sup>, PhD, Zhenghua Jiang<sup>15</sup>, BS, Yongxiu Zhang<sup>13</sup>, MD, Chao Dong<sup>13</sup>, MD, Yongchao Hu<sup>13</sup>,

9 MD, Lizhong Xie<sup>13</sup>, MD, Xugong Li<sup>16</sup>, PhD, Jianping Jiang<sup>13</sup>, MD, Huafen Zhu<sup>13</sup>, MPH, Wenxia Li<sup>1</sup>,

10 MSMT, Zhang Wen<sup>1</sup>, BSMT, Xiaofang Zheng<sup>13</sup>, BN, Yuanlong Sun<sup>4</sup>, MD, Xiaolu Zhou<sup>3</sup>, MD, Limin

11 Ding<sup>4</sup>, MD, Changhua Zhang<sup>1</sup>, MD, PhD, Wensheng Pan<sup>3</sup>, MD, Shuisheng Wu<sup>12</sup>, MD, Yiqun Hu<sup>2</sup>

12 , MD

13

14 1. Center for Digestive Disease, the Seventh Affiliated Hospital of Sun Yat-sen University, Shenzhen,

15 Guangdong, Province, P. R. China, 518107.

16 2. Department of Gastroenterology, Zhongshan Hospital Xiamen University, 201 Hubin South Road,

17 Xiamen, Fujian Province, P. R. China, 361004.

- 18 3. Zhejiang provincial people's hospital, People's Hospital of Hangzhou Medical College, Hangzhou,  
19 Zhejiang Province, P. R. China, 310014.
- 20 4. Tongxiang First People's Hospital, Tongxiang City, Zhejiang Province, P. R. China, 353000.
- 21 5. Jiying (XiaMen) Technology Co., LTD, Xiamen, Fujian Province, P. R. China, 361004.
- 22 6. Xiamen Cingene Science and technology co., LTD, Xiamen, Fujian Province, P. R. China, 361004.
- 23 7. State Key Laboratory of Marine Environmental Science, College of Ocean and Earth Sciences,  
24 Xiamen University, Xiamen, P.R. China, 361102.
- 25 8. Friedman Brain Institute, Icahn School of Medicine at Mount Sinai, New York, NY, USA, 10029.
- 26 9. Department of Immunobiology, Yale University School of Medicine, New Haven, CT 06510, USA
- 27 10. University of Pennsylvania Perelman School of Medicine, Philadelphia, USA.
- 28 11. The School of Pharmacy in Fujian Medical University, Fujian Province, P. R. China.
- 29 12. College of Pharmacy, Fujian University of Traditional Chinese Medicine, Fuzhou, Fujian, P.R.  
30 China, 350122.
- 31 13. Pucheng County Hospital of Traditional Chinese Medicine, Pucheng, Fujian Province, P. R. China,  
32 353400.
- 33 14. School of Life Sciences, Xiamen University, Xiamen, Fujian Province, P. R. China, 36110.
- 34 15. Department of Clinical Pharmacy, First Hospital of Nanping, Fujian Province, P. R. China, 314500
- 35 16. Department of Financial Engineering, Stevens Institute of Technology, Hoboken, NJ 07030, USA

36    **' Correspondence to:**

37    Changhua Zhang: Center for Digestive Disease, the Seventh Affiliated Hospital of Sun Yat-sen

38    University, No. 628, Zhenyuan Rd, Guangming (New) Dist, Shenzhen, Guangdong Province, P. R.

39    China, 518107. E-mail: zhchangh@mail.sysu.edu.cn. Tel: +86-755-81206101.

40    Shuisheng Wu: College of Pharmacy, Fujian University of Traditional Chinese Medicine, No.1

41    Qiuyang Road, Shangjie University Town, Fuzhou, Fujian, P.R. China, 350122. E-mail:

42    Wushuishengwss@163.com. Tel: +86-591-22861135.

43    Wensheng Pan: Zhejiang provincial people's hospital, People's Hospital of Hangzhou Medical College,

44    No. 158 of Shangtang Road, XiaCheng District, Hangzhou, Zhejiang Province, P. R. China, 310014.

45    E-mail: wspan223@163.com. Tel: +86-571-87666666.

46    Yiqun Hu: Department of Gastroenterology, Zhongshan Hospital Xiamen University, 201 Hubin South

47    Road, Xiamen, Fujian Province, P. R. China, 361004. E-mail: hyq0826@xmu.edu.cn. Tel:

48    +86-592-2590151.

49

50

51

52

53

54

## 55 **ABSTRACT**

56 Colorectal cancer (CRC) is the third in incidence and mortality<sup>1</sup> of cancer. Screening with colonoscopy  
57 has been shown to reduce mortality by 40-60%<sup>2</sup>. Challenge for screening indistinguishable  
58 precancerous and noninvasive lesion using conventional colonoscopy was still existing<sup>3</sup>. We propose to  
59 establish a propagable artificial intelligence assisted high malignant potential early CRC  
60 characterization system (ECRC-CAD). 4,390 endoscopic images of early CRC were used to establish  
61 the model. The diagnostic accuracy of high malignant potential early CRC was 0.963 (95% CI,  
62 0.941-0.978) in the internal validation set and 0.835 (95% CI, 0.805-0.862) in external datasets. It  
63 achieved better performance than the expert endoscopists. Spreading of ECRC-CAD to regions with  
64 different medical levels can assist in CRC screening and prevention.

## 65 **Introduction**

66 Colorectal cancer (CRC) is one of the most common malignant tumors in the globe<sup>4</sup>. “Cancer Statistics,  
67 2020” indicates that CRC ranks the third in incidence and mortality<sup>1</sup>. Accurate identification and  
68 treatment of early CRC have significantly reduced incidence and mortality<sup>5</sup>. However, early CRC is  
69 generally asymptomatic, and coloscopy allows direct visual inspection of the intestinal tract and  
70 same-session detection, biopsy, and subsequent removal of disease lesion. Several countries  
71 recommend that adults over the age of 50 should regularly screen CRC by coloscopy<sup>6,7</sup>. While

72 coloscopy is a kind of expert dependent examination, which can lead to missed diagnosis and  
73 misdiagnosis due to various causes, such as the experience of endoscopist, the interference during  
74 operation and inevitable interval of eye movement<sup>8</sup>. Computer assisted diagnose (CAD) system can  
75 solve above-mentioned problems.

76 In recent years, some Artificial Intelligence (AI)-based CAD systems have come into the pre-clinical  
77 application stage. However, the limitations of the research design (i.e. lack of external validation, not  
78 solving the critical clinical problems) lead to the consequence that the existing assistances are not really  
79 suitable for clinical practice directly<sup>9,10</sup>. In the field of gastrointestinal tumor, most studies focus on the  
80 detection of polyps and adenomas<sup>11,12</sup>, the staging of advanced cancer<sup>13</sup> and the optimizing of  
81 endoscopic operation<sup>14,15</sup>. Effects of these CAD systems in decreasing mortality rate of CRC need to be  
82 proven<sup>16</sup> by more clinical trials. Early gastrointestinal cancer diagnosis system that can directly  
83 decrease the occurrence of CRC is limited<sup>17</sup>, because the quantity of images from a single medical  
84 center is insufficient to support the establishment of the algorithm. Therefore, we aim to establish an  
85 early CRC CAD and malignant potential characteristic system (herein referred to as ECRC-CAD)  
86 based on standard white-light endoscopy (WLE), which can be clinically applied to different regions.

87 In this multi-center diagnostic clinical research, we establish an AI assisted early CRC diagnosis model  
88 using deep learning, which is based on images of different quality endoscopy from hospitals in  
89 different medical levels (i.e., rural, municipal, provincial) in China. Furthermore, ECRC-CAD can

90 identify intraepithelial neoplasm (IN), which is one of the most typical malignant precancerous  
91 conditions that can be differentiated by using image-enhanced endoscopy (IEE) and diagnosed by  
92 histology test. The clinical applicability of this model has been verified in the internal and external  
93 datasets collected retrospectively and another internal dataset collected prospectively.

## 94 **Methods**

### 95 **Study design and participants**

96 This study was a multi-center clinical diagnose research, which was completed in five hospitals at  
97 different medical levels across three provinces of China.

98 The workflow is shown in Figure 1. The first part is a case-control, retrospective research. All patients  
99 who underwent colonoscopy examination excepting for repeated examination in four hospitals from  
100 January 2016 to July 2019 are enrolled, including Zhongshan Hospital of Xiamen University (XMZSH)  
101 in Fujian, Zhejiang Provincial People's Hospital (ZJPH) in Zhejiang, the Seventh Affiliated Hospital of  
102 Sun Yat-sen University (SYSUSH) in Guangdong, and Pucheng County Traditional Chinese Medicine  
103 Hospital (PCTCRMH) in Fujian. Among them, SYSUSH started operation in July 2018. Patients who  
104 were diagnosed with early CRC by histopathological examination were selected. Pathological  
105 diagnosis was referred to the 4th WHO Classification of Tumors of Digestive System<sup>18</sup>. Early CRC in  
106 this article referred to precancerous conditions, in accordance with the requirements of the international  
107 standard. Patients with progressive colorectal cancer were excluded. Images of early CRC confirmed to

108 the database's including criteria (see in below) were included into case-control study, and were  
109 randomly assigned to the training set, evaluation & tuning set, and internal testing set in the ratio of  
110 8:1:1. All images of intraepithelial neoplasm (referred as IN-ECRC) were included to case group, and  
111 other early CRC without intraepithelial neoplasm (referred as NIN-ECRC) were randomly sample in  
112 corresponding quantity included to control group. ECRC-CAD was constructed and optimized using  
113 the first two data sets. To verify the veracity and clinical applicability of the model, we used validation  
114 datasets including images from the above internal testing set and another external testing set, which are  
115 consisted of images are according to the above criteria from Tongxiang Hospital (TXH) in Zhejiang.

116 The second part is a prospective research. The identification model officially completed the detection  
117 and model optimization of the above samples in September 2019, and was connected to the above five  
118 hospitals through the Internet. Then we prospectively collected the AI recognition results of all  
119 endoscopic center images in October 2019 and the first half of November 2019 from the above five  
120 hospitals, and extracted some endoscopic images of IN-ECRC and NIN-ECRC for senior doctors to  
121 identify.

122 Each participating institute has got ethical approval by independent ethics Committee according to the  
123 Helsinki declaration. The informed consent of retrospective cohort was exempted by the institutional  
124 review boards, causes it's the secondary use of clinical data without any intervention. In the  
125 prospective study, each patient was informed and signed up informed consent.

126 **Endoscopy and early CRC's image database**

127 Endoscopic images of five hospitals were captured by EC590WM, EC-600WM, EC-L590Z (WFujinon  
128 Corp, Saitama, Japan); V-70, PCF-H260AZI, CF-H260AI, CF-H290I, CF-HQ290I (Olympus Medical  
129 Systems, Tokyo, Japan); EC34-i10M , EG2990Z I (PENTAX medical, Tokyo, Japan). Each image of  
130 patients with early CRC was sequenced according to anatomical location, and screened by three  
131 endoscopy physicians. Exclusion criteria include: 1. The endoscopic anatomical location was not  
132 consistent with the pathological report, 2. Pictures were taken under IEE, 3. Pictures without any early  
133 CRC lesion, 4. Pictures was not confirmed to the sampling standard<sup>19</sup> summarized by our research team.  
134 All images in the database present at least one lesion, and multiple images might be taken for the same  
135 lesion, including differences of angle, distance, and extension of the intestinal wall. Images were saved  
136 in a jpeg format.

137 **Image Labeling**

138 Two senior endoscopists with more than 10 years of clinical experience, four residents and two  
139 assistants carried out image selection and labeling with blind method. The doctors were divided into  
140 three groups randomly, and at least one senior doctor in each group. The deep learning marking tool  
141 LabelMe<sup>20</sup> of Anaconda was used to mark the outline of disease lesion manually. Two physicians in the  
142 same group worked together. One was mainly responsible for drawing, and the other was mainly  
143 responsible for checking. Only when two physicians from the same group reached a consensus, the

144 labeling of the image could be finalized. After the first identification by ECRC-CAD, the misdiagnosed

145 images were double-checked so as to ensure the correctness and rationality of the results.

#### 146 **Construction and optimize of algorithm**

147 The ECRC-CAD's algorithm was based on the concept of full convolution networks<sup>21</sup> (FCN), which is

148 composed of classification module and post-processing module (Supplements p1-p2). The pattern

149 diagram was shown in Figure 2. Comparing with the classical CNN, this method can be adapted to

150 inputs with any size. In order to get an accurate boundary, we precisely outlined disease lesion of

151 images in establishing sets. The model contains one input and one output. The input of the model was

152 the image that contains the lesion. The output implemented a segmentation task that each pixel is

153 classified as background, intraepithelial neoplasm or other early CRC. Intraepithelial neoplasm was

154 abbreviated as "IN-ECRC", and the other early colorectal cancer neoplasm was abbreviated as

155 "NIN-ECRC". The labeling from histopathological examination was adopted as the gold standard in

156 training ECRC-CAD.

157 The implementation of AI-assisted precursor lesion identify model was fulfilled by using Python 3.7

158 (Python Software Foundation; [www.python.org/](http://www.python.org/)).

#### 159 **Algorithm testing and outcome measurement**

160 Three validation datasets were used to verify ECRC-CAD, which include internal datasets, external

161 datasets, and prospectively collected datasets. In the internal and external validate datasets, the

162 performance of ECRC-CAD was compared with the pathological golden standard of the corresponding  
163 tissues, and calculated statistic indicators on the individual images. When FCN detects early CRC from  
164 the input data of the validation image, the model outputs the lesion name. When the output result of the  
165 model is consistent with the pathological result, it is considered to be correct. In the prospective dataset,  
166 the performance was compared with histopathological result and expert at the same time. We randomly  
167 selected a subset of patients' images with histologically confirmed early CRC from the prospective  
168 collected datasets. Two experienced endoscopists were asked to complete independently the same test  
169 images together. These images' histology diagnosis is blinded to the two endoscopists. The diagnosis  
170 results of ECRC-CAD and experts were taken the patient as the unit, which is according with clinical  
171 requirements.

172 Sometimes, it's difficult to identify the whole images of disease lesion caused by the image quality and  
173 angle. When the model can identify even one picture of the cancer, it is considered as correct.

#### 174 **Statistical analysis**

175 In this study, descriptive analysis was used to describe the baseline characteristics of the enrolled  
176 subjects. Continuous variables were expressed by median (interquartile interval), dichotomous  
177 variables and grade variables that expressed by percentage. In order to evaluate the authenticity of  
178 ECRC-CAD, the diagnostic evaluation method was adopted. The evaluating indexes included  
179 Sensitivity, Specificity, Condolence, Positive predictive value (PPV), and Negative predictive value

180 (NPV). According to the above indexes, receiver operating characteristic (ROC) of different subgroups  
181 were drawn, and the area under the ROC curve (AUC) was calculated to evaluate the classification  
182 effect of this model on different subjects. More details are in the supplements p3. All statistical  
183 analyses in this study were based on the two-sided test 0.05 and performed through R software version  
184 3.6.0 (R Development Core Team).

## 185 **Results**

### 186 **Patient and image dataset information**

187 More than 6.2 million patients have done lower gastrointestinal tract in XMZSH, ZJRMH, SYSUSH,  
188 and PCRMH from January 2016 to August 2019. Almost 40% percent without any disease lesion were  
189 excluded. All participants diagnosed with IN-ECRC were enrolled in the model establishing sets, after  
190 quality control, 1923 images were enrolled, participants with NIN-ECRC corresponding in number of  
191 IN-ECRC were randomly extracted from other patients. The ratio of male to female is about 2.08:1.  
192 Age ranges from 20 to 86, and represent the right-skewed distribution (median age is 53.5). The  
193 baseline information of the establishing cohort and external cohort were listed in Table 1. Finally, in  
194 the stage of model establishment, 1923 images included in the case group, and 2467 images were  
195 included in the control group. In the model optimization stage, 490 images were included. In the  
196 verification stage, 189 images and 247 images were respectively collected in the above four hospitals  
197 as internal datasets. External datasets, including 960 images from 134 patients, were used to contract

198 and test ECRC-CAD. The prospectively collected datasets enrolled 672 patients, including 319  
199 IN-ECRC and 353 NIN-ECRC patients.

#### 200 **Performance of the precancerous detection model**

201 ECRC-CAD output results within 0.16 seconds and marks the boundary of disease lesion. The  
202 diagnosis result of each image was listed in supplementary material (eTable 1). The diagnostic  
203 accuracies of the internal validation dataset were 0.963 (95% CI, 0.941 to 0.978). External testing set  
204 only includes only IN-ECRC, which causes pathologists found that diagnostic criteria of NIN-ECRC in  
205 THX are not based on the 4th WHO Classification of Tumors of Digestive System. The sensitivity of  
206 ECRC-CAD in THX is 0.835 (95% IC, 0.805 to 0.862). The four indicators of the internal validation  
207 dataset is higher than 0.93. Similarly, a high AUC value (0.939) was also observed in the internal  
208 datasets (Figure 4). In the prospective study, the index of diagnosis accuracies was calculated in human  
209 units, which is more suitable for clinical needs. High accuracy (0.885, 95% CI, 0.859 to 0.907) was  
210 observed. The sensitivity and PPV were more than 0.90, and specificity and NPV were more than 0.85.  
211 The causes of misidentification are similarities, including incomplete exposure of disease lesions,  
212 concomitant other diseases, and some normal structures. The PPV (0.609, 95% IC, 0.454 to 0.745) and  
213 NPV (0.426, 95% IC, 0.303 to 0.559) were significantly lower for the expert endoscopists when  
214 compared with the AI-assisted model ( $P<0.0001$ ). Sensitivity and specificity between the endoscopic  
215 experts and the ECRC-CAD were visible.

216 This model has been successfully embedded in the above five hospitals, which is connected to the  
217 endoscopically connected computers through the Internet. Doctors and clinicians can identify the  
218 routine screenshots during the operation. The results of model recognition are displayed in the upper  
219 right corner of the screen in real time. In order to benefit more people, ECE-CAD is now available at:  
220 <http://123.57.221.125/#/home>. Home page is on display in Supplementary material (eFigure 2).  
221 Endoscopists can upload endoscopic images of suspected early CRC, and the system will give  
222 judgment in real time. Furthermore, we provided a set of WLE images of early CRC through open  
223 ports, which can help inexperienced endoscopist to familiar with it. The openness of this recognition  
224 model can also help endoscopists in less developed areas or those with low seniority to learn the  
225 recognition of early CRC (eFigure 3).

226 Both Asian and Western researchers consider that specific gross morphology, mucosal surface  
227 structure and microvascular structure or multi-changes of neoplasm have corresponding molecular  
228 characteristics<sup>22</sup>. We analyzed the microstructure feature of WLE, IEE in the same lesion taken from  
229 the same angle, and the association with features of H&E stained pathological image (eFigure 4).  
230 Combined with the published results (eTable 2), we proposed that the application of endoscopic images  
231 to predict molecular characteristics through endoscopic or pathology images in real-time is the future  
232 direction of “Image genomics”<sup>23</sup>.

## 233 **Discussion**

234 Overall, 1680 images of IN-ECRC and 2220 images of NIN-ECRC were used to establish and optimize  
235 ECRC-CAD. In order to ensure the clinical application of the model in underdeveloped regions, these  
236 images were collected from different medical level hospitals in China. Review published articles, it's  
237 the largest, multi-source endoscopic image database used to establish AI aided diagnose system in  
238 globe<sup>24</sup>. Furthermore, three clinical validation studies were conducted on the immediate clinical  
239 application value of ECRC-CAD, which showed high accuracy in the internal dataset (0.963). Liu et  
240 al<sup>25</sup> systematically reviewed the in-depth learning performance of diagnosis of disease from medical  
241 imaging. Of the 82 eligible researches from 2012 to 2019, only 25 have external validation. We  
242 avoided the issues mentioned above in this meta-analysis. The displayed ECRC-CAD can be extended  
243 to the external dataset from another rural hospital with a sensitivity of 0.835. This verification cohort  
244 could avoid highly accurate prediction which are caused by excessively spurious associations with the  
245 known outcome. However, case-control would not be representative of the general screening  
246 population<sup>26</sup>, and the predictor may not be directly applied to clinical practice. In this study, we  
247 validated ECRC-CAD in a prospective cohort, and ECRC-CAD and experts identified the disease's  
248 nature in real-time, respectively. The result showed that ECRC-CAD maintained perfect accuracy and  
249 specificity in prospective study, even better than expert endoscopist.

250 In clinical daily work, ECRC-CAD can assist endoscopist through increasing early CRC's detection  
251 rate, decreasing missed diagnosis rate (Figure S5). Endoscopy and clinical practice of operator have a

252 great influence on the detection and treatment of early cancer. A prospective study of UK<sup>27</sup> shows that  
253 the good performance of operating require skilled intubation operation and independent practice. While  
254 endoscopist in developed region can get more information about microstructure under IEE, which can  
255 increase diagnosis rate of early CRC by 10%-20%<sup>28</sup> comparing with WLE. However, early screening  
256 of neoplasm is mostly carried out in community hospitals with relatively low medical level, and the  
257 endoscopic equipment is relatively backward. Early CRC detection rate of ECRC-CAD has the same  
258 performance with IEE. Using ECRC-CAD enable people in lower medical level regions to get similar  
259 screening efficiency compared with subjects in developed regions.

260 Apart from assisting clinical decision, AI can make clinical path optimization possible<sup>23,29</sup>. The  
261 introduction of colorectal endoscopic submucosal dissection (ESD) increased the complete resection  
262 rate of early CRC<sup>30</sup> with minimally invasive trauma and low local recurrence possibility. High-grade  
263 IN without invasion or only superficial submucosal infiltration diagnosed by pathology examination is  
264 an indicator for ESD. The interval time between first endoscopic biopsy and pathology diagnosis is  
265 usually one week. At present, multi classification based on IEE<sup>31-33</sup> has been widely used to predict the  
266 risk of malignancy and invasiveness of CRC. Neoplasm confirm to indicators of malignant  
267 aggressiveness subtype according to these classifications can be removed during first endoscopic  
268 operation. It saved medical resources, and more important, absence of IEE or experts may increase  
269 metastasis of implanted cancer cell in natural cavity<sup>34</sup> due to incomplete resection. But there're some

270 limitations: Kudo, Sano classification is based on single observation index of pit or vessel pattern,  
271 NICE classification combining with gland and capillary pattern cannot differentiate IN from NIN, and  
272 all classifications need expert practice and IEE. ECRC-CAD can identify IN under WLE within 0.16  
273 second, which make up for the above deficiencies of present classification.

274 WL Bi<sup>23</sup> mentioned that characterization and monitoring are the future direction of AI in medical  
275 image. ECRC-CAD have realized characterization of precancerous lesion, and it can steadily monitor  
276 the progression of CRC without interference. However, with accumulation of medicine data  
277 preternaturally over time, AI will add rich layers of intelligence through combining molecular and  
278 pathological information with image-based findings. "Image genomics"<sup>23</sup> is the key to realize it,  
279 referring to the association of imaging characteristics with biological data, including specific molecular  
280 markers that are mainly based on immunohistochemical, or sequencing technology that are developed  
281 to direct personalized treatment planning. In lung cancers, researchers have established algorithm to  
282 predicted EGFR genotype using computed tomography image (MRI). Can endoscopic images be used  
283 in image genomics? We reviewed all researches of surface microstructure under endoscopy and  
284 molecular characteristics associated with colorectal neoplasms. These results indicate that that the AI  
285 have the potential of identify phenotypic and molecular specific pathological changes under WLE,  
286 causes of AI can extract a large number of features that cannot be observed by the human naked eyes.

287 The development of predicting multigroup tumor molecular markers through endoscopic images will  
288 paved the way for the future “one-step” clinical workflow with AI interventions.

289 The insufficiencies in this study includes: 1. ECRC-CAD can’t increase adenoma detection rate (ADR),  
290 because it’s based on static image taken by endoscopist. We’ve explored a CAD based on video, and  
291 the clinical validation is processing. 2. The external validation set is not included with NIN-ECRC. We  
292 are reassessing this part of cases by two expert histopathologists, to add a complete evaluation to this  
293 model. 3. Sample of high-grade IN is limited for making differentiation of ECRC-CAD in low or  
294 high-grade of IN. 4. We just focus on identifying IN-ECRC from NIN-ECRC, which can’t distinguish  
295 between sessile serrated lesions and other lesions. However, about 80% of sporadic CRC develop from  
296 IN<sup>18</sup>, removal of which may decrease the incidence of colorectal cancer by 53%. 5. The prospective  
297 validation is not a randomized controlled trial (RCT). We’re planning to proceed with subsequent RCT  
298 studies in more centers. 6. We just put forward the endoscopic image that can be used to predict  
299 molecular subtype, but ECRC-CAD cannot identify surface microstructure yet. Considering the clinical  
300 applicability, the model was constructed using images taken by WLE in this study, which were not  
301 suitable for micro-structure classification. In subsequent RCT studies, high-resolution WLE and IEE  
302 images of early neoplasm will be prospectively collected to construct the classification model for  
303 microstructure.

304 This is an exploratory study on identification and diagnosis of early cancers that could be applied to  
305 other organs of digestion system, such as the stomach and esophagus.

306

### 307 **Acknowledgement**

308 This research was supported by Major Science and Technology Project of Zhejiang Provincial  
309 (2020C03030), Natural Science Foundation of Fujian Province (2019-CXB-31), Science and  
310 technology program of Guangdong Province (2016A020213002), and National Natural Science  
311 Foundation of China (81773956). We would like to thank: (1) Yonghe Zhou, Kunping Hang for  
312 coordinating the data in the primary hospitals; (2) Tonghai Dou, Ph.D, Chuncheng Cheng, ZI CHONG  
313 KUO providing valuable advice; and Volunteer Joey Yau helps in data collation; (3) The Pucheng  
314 county health administration has provided assistance to primary hospitals; (4)The families of all the  
315 participants provided spiritual encouragement and material support, allowing researchers to continue  
316 their experiments in the most difficult times.

317

### 318 **Contributors**

319 Yiqun Hu is general manager the of the project. Hesong Qiu is the project coordinator and participates  
320 in the optimization of research design. Sijun Meng, Wangyue Wang, Yu Zhang, Zhaofang Han,  
321 Wenjuan Qin, Yuhuan Zhong, Yi Zhang, Zhenghua Jiang, Yongxiu Zhang, Chao Dong, Yongchao Hu,

322 Lizhong Xie, Jianping Jiang, Huafen Zhu, Wenxia Li, Zhang Wen, Xiaofang Zheng, Yuanlong Sun,  
323 Xiaolu Zhou, Limin Ding have contributed in participants' enrollment, imaging collecting and quality  
324 control. Yueping Zheng, Ruizhang Su, Siqi Wu, Yemei Bu, Xiaofang Zheng have classified and  
325 integrated data. Hang Xiao and Chen Yang are responsible for algorithm establishing and optimizing.  
326 Sijun Meng, Wen Zhang, Lichong Yan, Haineng Xu, and Xugong Li contribute to manuscript writing.  
327 Ruizhang Su, Yemei Bu, Wenjuan Qin, Hong Chen, Wensheng Pan, Yiqun Hu were organized and  
328 labeled photos. Yiqun Hu, Wensheng Pan, Hong Chen identified the IN-ECRC as expert endoscopist.  
329 Shuisheng Wu, Wensheng Pan and Changhua Zhang's contributed equally in the project.  
330 The corresponding author is Changhua Zhang, Shuisheng Wu, Wensheng Pan, Yiqun Hu. According to  
331 the author ranking, Hesong Qiu and the previous author are first co-authors, Xugong Li and the  
332 previous author are second co-authors, the others is the third co-authors.

333

### 334 **Ethical approval**

335 This study was approved by the medical ethic committee of each participants (IRB serial number:  
336 XMZSYKY\_ER No.2019023).

337

### 338 **Declaration of interests**

339 We declare no competing interests.

340

341 **Reference:**

342 1. Siegel, R.L., Miller, K.D. & Jemal, A. Cancer statistics, 2020. *CA: A Cancer*

343 *Journal for Clinicians* **70**, 7-30 (2020).

344 2. Brenner, H., Stock, C. & Hoffmeister, M. Effect of screening sigmoidoscopy

345 and screening colonoscopy on colorectal cancer incidence and mortality:

346 systematic review and meta-analysis of randomised controlled trials and

347 observational studies. *BMJ (Clinical research ed.)* **348**, g2467-g2467 (2014).

348 3. Su, M.-Y., *et al.* Comparative study of conventional colonoscopy,

349 chromoendoscopy, and narrow-band imaging systems in differential diagnosis

350 of neoplastic and nonneoplastic colonic polyps. *The American journal of*

351 *gastroenterology* **101**, 2711-2716 (2006).

352 4. Bray, F., *et al.* Global cancer statistics 2018: GLOBOCAN estimates of

353 incidence and mortality worldwide for 36 cancers in 185 countries. *CA: a*

354 *cancer journal for clinicians* **68**, 394-424 (2018).

355 5. Lin, J.S., *et al.* Screening for Colorectal Cancer: Updated Evidence Report and

356 Systematic Review for the US Preventive Services Task Force. *JAMA* **315**,

357 2576-2594 (2016).

- 358 6. Wolf AMD, F.E., Church TR, et al. . Colorectal cancer screening for  
359 average-risk adults: 2018 guideline update from the American Cancer Society.  
360 *CA Cancer J Clin* **68(4)**, 250–281 (2018).
- 361 7. Wender RC, B.O., Fedewa SA, Gansler T, Smith RA. . A blueprint for cancer  
362 screening and early detection: Advancing screening's contribution to cancer  
363 control. *CA Cancer J Clin* **69(1)**, 50–79 (2019).
- 364 8. Lee, J., *et al.* Risk factors of missed colorectal lesions after colonoscopy.  
365 *Medicine (Baltimore)* **96**, e7468-e7468 (2017).
- 366 9. Rajkomar A, D.J., Kohane I. Machine Learning in Medicine. *N Engl J Med*  
367 **380(14)**, 1347–1358 (2019).
- 368 10. AI diagnostics need attention. *Nature* **555(7696)**, 285 (2018).
- 369 11. Byrne, M.F., *et al.* Real-time differentiation of adenomatous and hyperplastic  
370 diminutive colorectal polyps during analysis of unaltered videos of standard  
371 colonoscopy using a deep learning model. *Gut* **68**, 94-100 (2019).
- 372 12. Wang, P., *et al.* Real-time automatic detection system increases colonoscopic  
373 polyp and adenoma detection rates: a prospective randomised controlled study.  
374 *Gut* **68**, 1813-1819 (2019).

- 375 13. Zhu Y, W.Q., Xu MD, et al. Application of convolutional neural network in  
376 the diagnosis of the invasion depth of gastric cancer based on conventional  
377 endoscopy. *Gastrointest Endosc* **89**(4), 806–815.e801. (2019).
- 378 14. Wu, L., *et al.* Randomised controlled trial of WISENSE, a real-time quality  
379 improving system for monitoring blind spots during  
380 esophagogastroduodenoscopy. *Gut* **68**, 2161-2169 (2019).
- 381 15. Wu, L., *et al.* A deep neural network improves endoscopic detection of early  
382 gastric cancer without blind spots. *Endoscopy* **51**, 522-531 (2019).
- 383 16. Rees, C.J. & Koo, S. Artificial intelligence - upping the game in  
384 gastrointestinal endoscopy? *Nature reviews. Gastroenterology & hepatology*  
385 **16**, 584-585 (2019).
- 386 17. de Lange, T., Halvorsen, P. & Riegler, M. Methodology to develop machine  
387 learning algorithms to improve performance in gastrointestinal endoscopy.  
388 *World J Gastroenterol* **24**, 5057-5062 (2018).
- 389 18. Bosman, F.T., Carneiro, F., Hruban, R.H. & Theise, N.D. *WHO classification*  
390 *of tumours of the digestive system*, (World Health Organization, 2010).
- 391 19. Zheng, Y., *et al.* Setting Standards to Promote Artificial Intelligence in Colon  
392 Mass Endoscopic Sampling. *medRxiv*, 19008078 (2019).

- 393 20. Russell, B.C., Torralba, A., Murphy, K.P. & Freeman, W.T. LabelMe: A  
394 Database and Web-Based Tool for Image Annotation. *International Journal of*  
395 *Computer Vision* **77**, 157-173.
- 396 21. Shelhamer, E., Long, J. & Darrell, T. Fully Convolutional Networks for  
397 Semantic Segmentation. *IEEE Transactions on Pattern Analysis and Machine*  
398 *Intelligence* **39**, 640-651 (2017).
- 399 22. Suzuki, H., Yamamoto, E., Yamano, H.-O., Nakase, H. & Sugai, T. Integrated  
400 Analysis of the Endoscopic, Pathological and Molecular Characteristics of  
401 Colorectal Tumorigenesis. *Digestion* **99**, 33-38 (2019).
- 402 23. Bi, W.L., *et al.* Artificial intelligence in cancer imaging: Clinical challenges  
403 and applications. *CA: a cancer journal for clinicians* **69**, 127-157 (2019).
- 404 24. Ahmad, O.F., *et al.* Artificial intelligence and computer-aided diagnosis in  
405 colonoscopy: current evidence and future directions. *Lancet Gastroenterol*  
406 *Hepatol* **4**, 71-80 (2019).
- 407 25. Liu, X., *et al.* A comparison of deep learning performance against health-care  
408 professionals in detecting diseases from medical imaging: a systematic review  
409 and meta-analysis. *The Lancet Digital Health* **1**, e271-e297 (2019).

- 410 26. Zhou, Q., Cao, Y.-H. & Chen, Z.-H. Optimizing the study design of clinical  
411 trials to identify the efficacy of artificial intelligence tools in clinical practices.  
412 *EClinicalMedicine* **16**, 10-11 (2019).
- 413 27. Siau, K., Hawkes, N.D., Dunckley, P. & Valori, R.M. Impact of fellowship  
414 training level on colonoscopy quality and efficiency metrics: a United  
415 Kingdom perspective. *Gastrointestinal endoscopy* **89**, 441-442 (2019).
- 416 28. Guo, T.-J., *et al.* Diagnostic performance of magnifying endoscopy with  
417 narrow-band imaging in differentiating neoplastic colorectal polyps from  
418 non-neoplastic colorectal polyps: a meta-analysis. *Journal of gastroenterology*  
419 **53**, 701-711 (2018).
- 420 29. Rajkomar, A., Dean, J. & Kohane, I. Machine Learning in Medicine. *The New*  
421 *England journal of medicine* **380**, 1347-1358 (2019).
- 422 30. Sakamoto, T., *et al.* Endoscopic submucosal dissection for colorectal  
423 neoplasms: a review. *World journal of gastroenterology* **20**, 16153-16158  
424 (2014).
- 425 31. Kudo, S., *et al.* Diagnosis of colorectal tumorous lesions by magnifying  
426 endoscopy. *Gastrointest Endosc* **44**, 8-14 (1996).

427 32. Sano, Y., *et al.* Magnifying observation of microvascular architecture of  
428 colorectal lesions using a narrow-band imaging system. *Digestive endoscopy*  
429 **18**, S44-S51 (2006).

430 33. Hayashi, N., *et al.* Endoscopic prediction of deep submucosal invasive  
431 carcinoma: validation of the narrow-band imaging international colorectal  
432 endoscopic (NICE) classification. *Gastrointestinal endoscopy* **78**, 625-632  
433 (2013).

434 34. Lee, H.J., *et al.* Is endoscopic submucosal dissection safe for papillary  
435 adenocarcinoma of the stomach? *World journal of gastroenterology* **21**,  
436 3944-3952 (2015).

437

438

439

440

441

442

443

444

445

446

447

## 448 **FIGURE LEGENDS**

### 449 **Figure 1. Workflow of establishment and valuation of ECRC-CAD**

450 The flow chart shows the construction and validation process and committed steps of ECRC-CAD.

### 451 **Figure 2. Diagram of ECRC-CAD**

452 Algorithm of ECRC-CAD is based on FCN8. Score of IN-ECRC+ score of NIN-ECRC=1, If score of

453 IN-ECRC >score of NIN-ECRC, we recognize it as IN-ECRC, if score of NIN-ECRC>score of

454 IN-ECRC, we recognize it as NIN-ECRC.

### 455 **Figure 3. Demonstration of ECRC-CAD's extraction and characterization results**

456 The left image of each pair is the original image under the endoscope, the right image of each pair is

457 the disease lesion extracted by ECRC-CAD. Predict result was listed under each pair of images. The

458 "Prediction" result represents the type of extracted lesion identified by ECRC-CAD, the "confidence"

459 represents the score that were calculated by ECRC-CAD.

### 460 **Figure 4. Receiver operating characteristic curves of ECRC-CAD**

461 ECRC-CAD performance on the internal validate sets (436 images). AUC indicates area under the

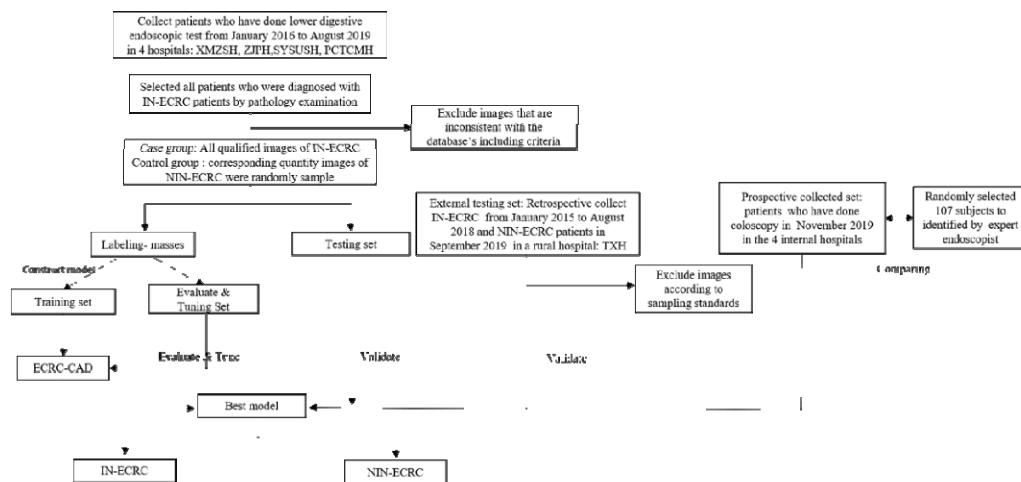
462 receiver operating characteristic curve.

463

464

465 **FIGURES**

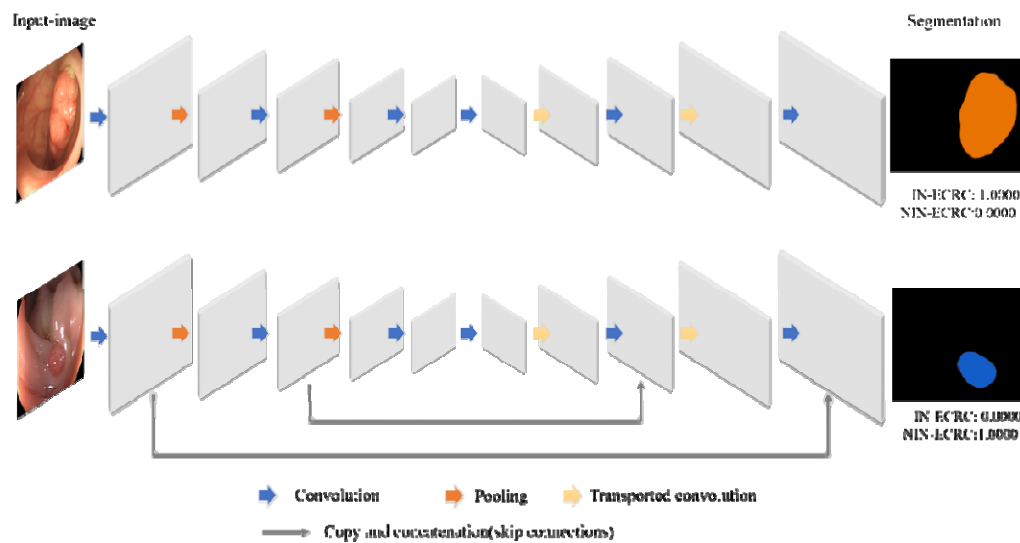
466 **Figure 1. Workflow of establishment and valuation of ECRC-CAD**



467

468

469 **Figure 2. Diagram of ECRC-CAD**



470

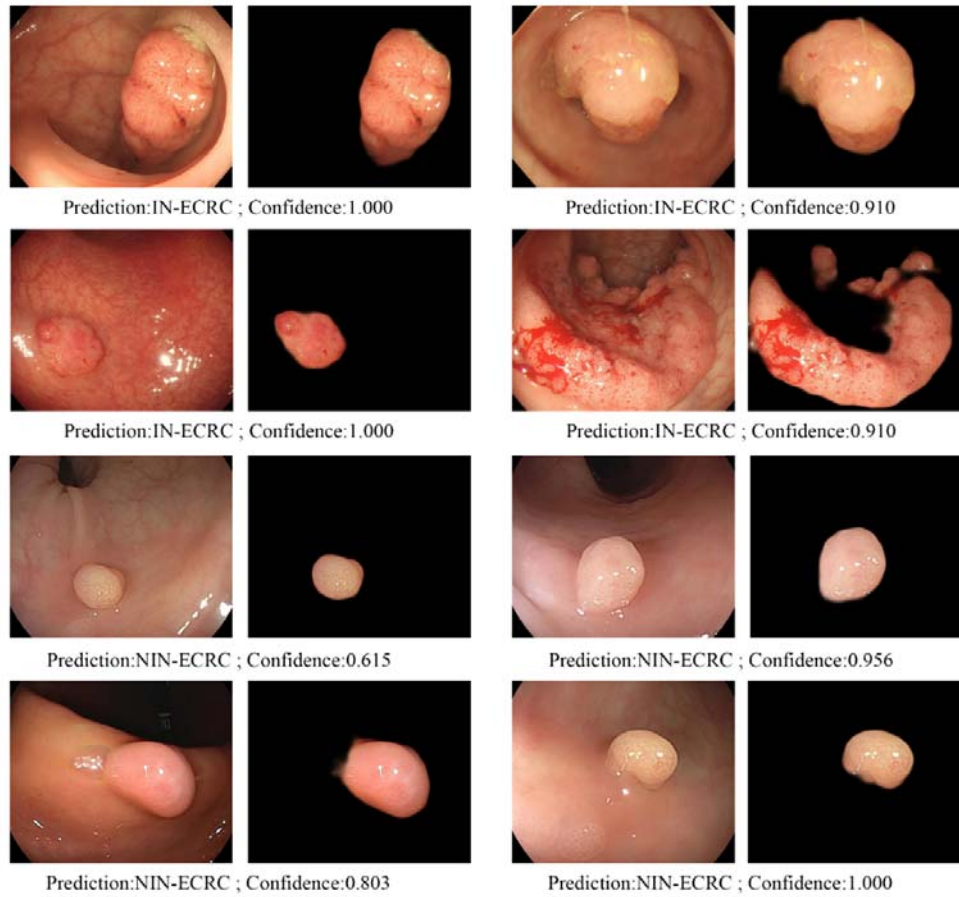
471

472

473

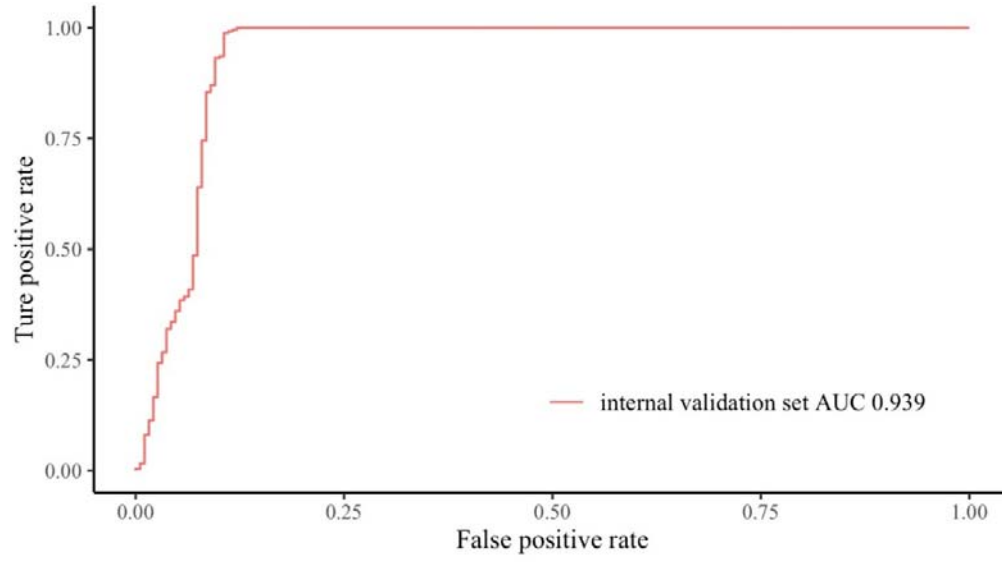
474 **Figure 3. Demonstration of ECRC-CAD's extraction and characterization**

475 **results**



476

477 **Figure 4. Receiver operating characteristic curves of ECRC-CAD**



478

479 **Table 1. Baseline information**

		Establish cohort			Validate cohort		Expert
		Establishing set (unit: image)	Evaluate & Tuning set (unit: image)	Internal testing set (unit: image)	External testing set (unit: image)	Prospective testing set (unit: person)	endoscopists (unit: person)
Sum of subjects		3464	490	436	674	454	107
Stage	IN-ECRC	1491	243	189	674	98	63
	NIN-ECRC	1973	247	247	NaN	353	44

480

481

482

483

484

485

486

487

488

489 **Table 2. Performance of ECRC-CAD in different validation dataset and expert endoscopist in distinguishing IN-ECRC and NIN-ECRC**

	Internal testing set	External testing set	Prospective testing set	Expert endoscopist	ECRC-CAD vs Endoscopist*
Accuracy (95% CI)	0.963 (0.941-0.978)	0.835(0.805-0.862)	0.885 (0.859-0.907)	0.505 (0.411-0.598)	<i>P</i> <0.0001
Sensitivity (95% CI)	0.937 (0.889-0.965)	0.835(0.805-0.862)	0.915 (0.878-0.942)	0.444 (0.321-0.575)	<i>P</i> <0.0001
Specificity (95% CI)	0.984 (0.956-0.995)	NaN	0.858 (0.817-0.892)	0.591 (0.433-0.733)	<i>P</i> <0.0001
PPV (95% CI)	0.978 (0.941-0.993)	NaN	0.854 (0.811-0.887)	0.609 (0.454-0.745)	<i>P</i> <0.0001
NPV (95% CI)	0.953 (0.917-0.974)	NaN	0.918 (0.882-0.944)	0.426 (0.303-0.559)	<i>P</i> <0.0001

490 \*McNemar's test